Journal of Alloys and Compounds 702 (2017) 303–308

Contents lists available at ScienceDirect

Journal of Alloys and Compounds

journal homepage: http://www.elsevier.com/locate/jalcom

Synthesis and characterization of lanthanide-based coordination polymers for highly selective and sensitive luminescent sensor for Pb^{2+} over mixed metal ions

Chen Lian, Yi Chen, Sai Li, Meng-yang Hao, Feng Gao, Li-rong Yang*

Henan Key Laboratory of Polyoxometalate, Institute of Molecule and Crystal Engineering, College of Chemistry and Chemical Engineering, Henan University, Kaifeng 475004, PR China

ARTICLE INFO

Article history:
Received 11 October 2016
Received in revised form
18 January 2017
Accepted 22 January 2017
Available online 25 January 2017

Keywords:
Coordination polymers
Luminescent sensor
Lanthanide contraction
Magnetic analysis
Metal-organic frameworks

ABSTRACT

Three novel coordination polymers, namely, $\{[Pr(TTTPC)\cdot(H_2O)_2]\cdot 2Cl\cdot NO_3\cdot 4H_2O\}_n$ (**I**), $\{[Gd(TTTPC)\cdot(H_2O)_2]\cdot 2Cl\cdot NO_3\cdot 4H_2O\}_n$ (**II**) and $\{[Yb(TTTPC)\cdot(H_2O)_2]\cdot 3Cl\cdot NO_3\cdot 0.5DMA\cdot 6H_2O\}_n$ (**III**) were synthesized in conventional aqueous solutions with H_3TTTPC ligands (H_3TTTPC = 1,1′,1″-(2,4,6-trimethylbenzene-1,3,5-triyl(methylene))-tris(pyridine-4-carboxylic acid), DMA = *N*,*N*-dimethylacetamide) and characterized by infrared spectrometry and single crystal X-ray diffraction. Experimental results show that these MOFs are isomorphous and isostructural, containing the unit of cavate 14-membered cages ($Pr_2(OCO)_4$), based on which to generate a one-dimensional (1D) infinite linear metallic chain through the linkage of two COO^- groups that are further interlinked reciprocally to polymerize into three-dimensional (3D) porous frameworks. Coordination polymer **III** shows remarkable selectivity toward Pb^{2+} and it can be considered as potential selective luminescent probes for Pb^{2+} ion. Additionally, magnetic analysis indicates coordination polymer **I** presents antiferromagnetism. Besides, lanthanide contraction effect exists in as-synthesized coordination polymers.

1. Introduction

Much effort has been focused on coordination polymers for decades, this particular class of crystalline materials by rational design strategies typically present a high degree of structural and incomparable functional tunability [1–4], which make them not only own various fascinating architectures but also possess potential practical applications in the fields of gas storage and separation, selective luminescent probes, magnetism, heterogeneous catalysis, electrical conductivity and nonlinear optic etc. [5–14]. Lanthanide-based coordination polymers, especially the applications of which for sensing metal ions and small organic molecule, have been attracting great deal of attention. On one hand, lanthanide coordination polymers have highly localized 4f electrons which provide the possibility of f-f transitions and closely relate to the emission behavior of lanthanide ions with high quantum yields in a narrow wavelength range, and so as to make them have special photochemical properties that other compounds are rarely available [15–17]. On the other hand, lanthanide ions possess larger radius and higher affinity for hard donor centers and ligands with hybrid oxygen and nitrogen atoms, which are beneficial to the construction of coordination polymers [18–21].

Coordination polymers may display diverse structure and different connecting modes in various reaction conditions such as metal sources, pH value, temperature, reactant concentration and solvents. Moreover, electing building blocks including suitable structural and geometrical information that may code for an expected underlying net prior to the assembly process plays an important role in obtaining coordination polymers with desired structure and excellent properties [22–25]. Naturally, multidentate organic ligands like polycarboxylic acids which contain rich coordination modes as bridging ligands and high affinity of metal ions for the oxygen and nitrogen atoms are most widely used for the construction of coordination polymers, this assembly system is potentially in favor of polymerizing into extended open frameworks and then forming multi-dimensional coordination polymers [26–30].

In view of recent important progress as well as our longstanding research on the structure and physical properties of organic lanthanide coordination polymers, various polycarboxylic acids

* Corresponding author.
E-mail address: lirongyang@henu.edu.cn (L.-r. Yang).

http://dx.doi.org/10.1016/j.jallcom.2017.01.260
0925-8388/

have been employed in the experiments to explore the structure and properties of coordination polymers, looking forward to increase the possibility of practical applications [31–36]. In this work, we choose 1,1′,1″-(2,4,6-trimethylbenzene-1,3,5-triyl(methylene))-tris(pyridine-4-carboxylic) (H_3TTTPC) as bridging ligand which features a combination of rigidity and flexibility that allows H_3TTTPC to link metal ions in different directions thereby supporting the construction of multidimensional coordination polymers [37–40], preparing three 3D coordination polymers formulated as $\{[Pr(TTTPC)\cdot(H_2O)_2]\cdot 2Cl\cdot NO_3\cdot 4H_2O\}_n$ (**I**), $\{[Gd(TTTPC)\cdot(H_2O)_2]\cdot 2Cl\cdot NO_3\cdot 4H_2O\}_n$ (**II**) and $\{[Yb(TTTPC)\cdot(H_2O)_2]\cdot 3Cl\cdot NO_3\cdot 0.5DMA\cdot 6H_2O\}_n$ (**III**), and report the synthesis, crystal structures, magnetism and luminescent properties for sensing metal ions.

2. Experimental section

2.1. Materials and physical measurements

All chemicals were commercially purchased and used without further purification. IR spectra in the range of 400–4000 cm^{-1} were obtained with an AVATAR 360 FT-IR spectrometer (KBr pellets were used). The crystal structure was determined with a Bruker Smart CCD X-ray single-crystal diffractometer. Excitation and emission spectra were recorded with an F-7000 FL spectrofluorometer at room temperature. Magnetic susceptibility measurements were conducted with a Quantum Design MPMS-5 magnetometer in the temperature range of 2.0–300.0 K. Thermogravimetric (TG) analyses were conducted with a Perkin-Elmer TGA7 system under flowing N_2 stream (flow rate 40 mL/min) at a heating rate of 10 K/min.

2.2. Synthesis of the coordination polymers *I*, *II* and *III*

2.2.1. Synthesis of *I*

$\{[Pr(TTTPC)\cdot(H_2O)_2]\cdot 2Cl\cdot NO_3\cdot 4H_2O\}_n$ (**I**) was synthesized from the reaction mixture of 1,1′,1″-(2,4,6-trimethylbenzene-1,3,5-triyl(methylene))-tris(pyridine-4- carboxylic) and praseodymium nitrate at a molar ratio of 1:1 (0.1 mmol: 0.1 mmol) in 10 mL mixed solvent of DMA and water (volume ratio 2 mL: 8 mL). The resultant mixture was homogenized by stirring for 120 min at 80 °C and then cooling to room temperature. Filtering the mixture into a 50 mL flat bottom breaker and volatiling at room temperature. After 60 days, the product was washed with DMF and absolute ether, and then dried to afford colorless block-shaped crystals suitable for X-ray diffraction analysis. IR data (KBr pellet, cm^{-1}): 3394(m), 3111(m), 1608(s), 1565(s), 1409(s), 1251(w), 1213(w), 1133(m), 1080(w), 1043(w), 876(w), 774(m), 695(w), 643(w), 559(w), 413(w).

2.2.2. Synthesis of *II* and *III*

Coordination polymers **II** and **III** were prepared by the identical experimental procedures to that of **I** except that praseodymium nitrate was replaced by gadolinium nitrate and yttrium nitrate, respectively.

For $\{[Gd(TTTPC)\cdot(H_2O)_2]\cdot 2Cl\cdot NO_3\cdot 4H_2O\}_n$ (**II**). IR data (KBr pellet, cm^{-1}): 3402(m), 3110(m), 1636(s), 1568(s), 1450(m), 1387(s), 1254(m), 1200(w), 1158(w), 1131(m), 1043(m), 878(w), 861 (w), 803(w), 775(m), 693(m), 634(m), 543(w), 461(w), 399(w).

For $\{[Yb(TTTPC)\cdot(H_2O)_2]\cdot 3Cl\cdot NO_3\cdot 0.5DMA\cdot 6H_2O\}_n$ (**III**). IR data (KBr pellet, cm^{-1}): 3411(m), 3111(m), 1637(s), 1568(s), 1448(m), 1387(s), 1242(m), 1198(w), 1157(w), 1130(m), 1042(m), 878(w), 857(w), 804(w), 771(m), 692(m), 635(m), 613(w), 546(w), 462(w).

2.3. Crystallographic data collection and refinement

Single-crystal diffraction data **I**, **II** and **III** were collected suitable single crystals of the coordination polymers on a Bruker Smart CCD X-ray single-crystal diffractometer with graphite monochromated MoKα-radiation ($\lambda = 0.71073$ Å). All independent reflections were collected in a range of 1.703–28.319° for coordination polymer **I**, 2.193–28.263° for coordination polymer **II** and 1.698–28.302° for coordination polymer **III** (determined in the subsequent refinement). Multi-scan empirical absorption corrections were applied to the data using the SADABS. The crystal structure was solved by direct methods and Fourier synthesis. Positional and thermal parameters were refined by the full-matrix least-squares method on F^2 using the SHELXTL software package. The final least-square cycle of refinement gave $R_1 = 0.0540$, $wR_2 = 0.1503$ for coordination polymer **I**, $R_1 = 0.0411$ $wR_2 = 0.1161$ for coordination polymer **II** and $R_1 = 0.0427$, $wR_2 = 0.11909$ for coordination polymer **III**, the weighting scheme $w = 1/[\sigma^2(F_0^2)+(0.1090P)^2]$ for coordination polymer **I** and $w = 1/[\sigma^2(F_0^2)+(0.0783P)^2+2.0330P]$ for coordination polymer **II** and $w = 1/[\sigma^2(F_0^2)+(0.0806P)^2+2.8705P]$ for coordination polymer **III**, where $P = (F_0^2 + 2F_c^2)/3$. The crystallographic data, selected bond lengths and bond angles for coordination polymers **I**, **II** and **III** are listed in Table 1 and Table S1, respectively. CCDC 1495825, 1495826 and 1495824 correspond to **I**, **II** and **III**, respectively.

3. Results and discussion

3.1. FT-IR spectroscopy

Coordination polymers are insoluble in common solvents such as CH_3COCH_3, CH_3CH_2OH, and $CH_3CH_2OCH_2CH_3$, but they are slight soluble in CH_3OH, DMSO, and DMF. The structures of the coordination polymers are identified by FT-IR and X-ray analyses. The FT-IR spectra of the three as-synthesized coordination polymers are similar. The strong and broad absorption bands in the ranges of 3411–3394 cm^{-1} are assigned to the stretching vibrations of $\nu_{(O\text{-}H)}$ in water molecules in coordination and lattice forms [41,42]. Some other strong absorption bands in the region of 1637–1565 cm^{-1} and 1448–1387 cm^{-1} may be ascribed to the asymmetric (COO^-) and symmetric (COO^-) stretching of carboxyl groups of H_3TTTPC ligands in **I**–**III**. The values of $\Delta[\nu_{as}-\nu_s]$ are about 199–250 cm^{-1}, which indicate that the carboxyl groups are coordinated with the metal ions *via* bidentate-bridging mode. The absence of the characteristic bands ranging from 1690 to 1730 cm^{-1} indicates that the H_3TTTPC ligands are completely deprotonated in the form of $TTTPC^{3-}$ anions upon reaction with the metal ions. The $\delta_{O\text{-}C\text{-}O}$ vibration in plane occurs as sharp peaks in the range of 690–780 cm^{-1} [43–45]. The same conclusions are also supported by the results obtained from X-ray diffraction measurements.

3.2. Structural description of the coordination polymers

The Single crystal X-ray diffraction analysis reveals that the three-dimensional coordination polymers of **I**, **II** and **III** are isomorphous and isostructural, crystallizing in the triclinic space group *P*-1. Hence, coordination polymer **I** is selected as an example to describe the formation of 3D structure in detail. In coordination polymer **III**, the asymmetric unit contains one crystallographically independent Pr (III) center, six individual $TTTPC^{3-}$ ligands, as well as two coordinated water molecules. Pr1 is eight-coordinated and surrounded by eight oxygen atoms (O1, O2, O3, O4, O5, and O6) belonging to six different $TTTPC^{3-}$ ligands and two terminal water molecules (O1w and O2w) to exhibit the bicapped trigonal prism geometry, as illustrated in Fig. 1a and Fig. S1. $TTTPC^{3-}$ ligand adopts

Table 1
Summary of crystallographic data for **I**, **II** and **III**.

Compound	I	II	III
Empirical formula	$C_{30}H_{39}Cl_2N_4O_{15}Pr$	$C_{30}H_{39}Cl_2N_4O_{15}Gd$	$C_{32}H_{48.5}Cl_3N_{4.5}O_{17.5}Yb$
Formula weight	907.46	923.80	1055.64
Temperature/K	293	296.15	296.15
Crystal system	triclinic		
Space group	*P*-1		
a/Å	9.5285(19)	9.5522(4)	9.4755(4)
b/Å	12.760(3)	12.9330(6)	13.0729(6)
c/Å	18.896(4)	18.7637(9)	18.4582(9)
α/°	106.72(3)	106.9720(10)	107.5060(10)
β/°	98.91(3)	98.2490(10)	96.5740(10)
γ/°	98.59(3)	97.7940(10)	98.2310(10)
Volume/Å^3	2127.6(8)	2155.23(17)	2127.82(17)
Z	2		
ρ_{calc} g/cm^3	1.416	1.424	1.648
μ/mm^{-1}	1.334	1.725	2.462
F(000)	920	930	1066
Radiation/Å	MoKα ($\lambda = 0.71073$)		
2θ range for data collection/°	3.406–56.638	4.386–56.526	3.396–56.604
Index ranges	$-12 \le h \le 12$, $-16 \le k \le 15$, $-24 \le l \le 25$	$-10 \le h \le 12$, $-17 \le k \le 13$, $-24 \le l \le 24$	$-8 \le h \le 12$, $-17 \le k \le 16$, $-23 \le l \le 24$
Reflections collected	13449	13660	13499
Independent reflections	9789 [$R_{int} = 0.0314$, $R_{sigma} = 0.0617$]	9889 [$R_{int} = 0.0174$, $R_{sigma} = 0.0412$]	9792 [$R_{int} = 0.0204$, $R_{sigma} = 0.0446$]
Data/restraints/parameters	9789/48/499	9889/57/500	9792/96/584
Goodness-of-fit on F^2	1.050	1.058	1.061
Final *R* indexes [$I \ge 2\sigma(I)$]	$R_1 = 0.0540$, w$R_2 = 0.1503$	$R_1 = 0.0411$, w$R_2 = 0.1161$	$R_1 = 0.0427$, w$R_2 = 0.11909$
Final *R* indexes [all data]	$R_1 = 0.0647$, w$R_2 = 0.1609$	$R_1 = 0.0487$, w$R_2 = 0.1253$	$R_1 = 0.0477$, w$R_2 = 0.1236$

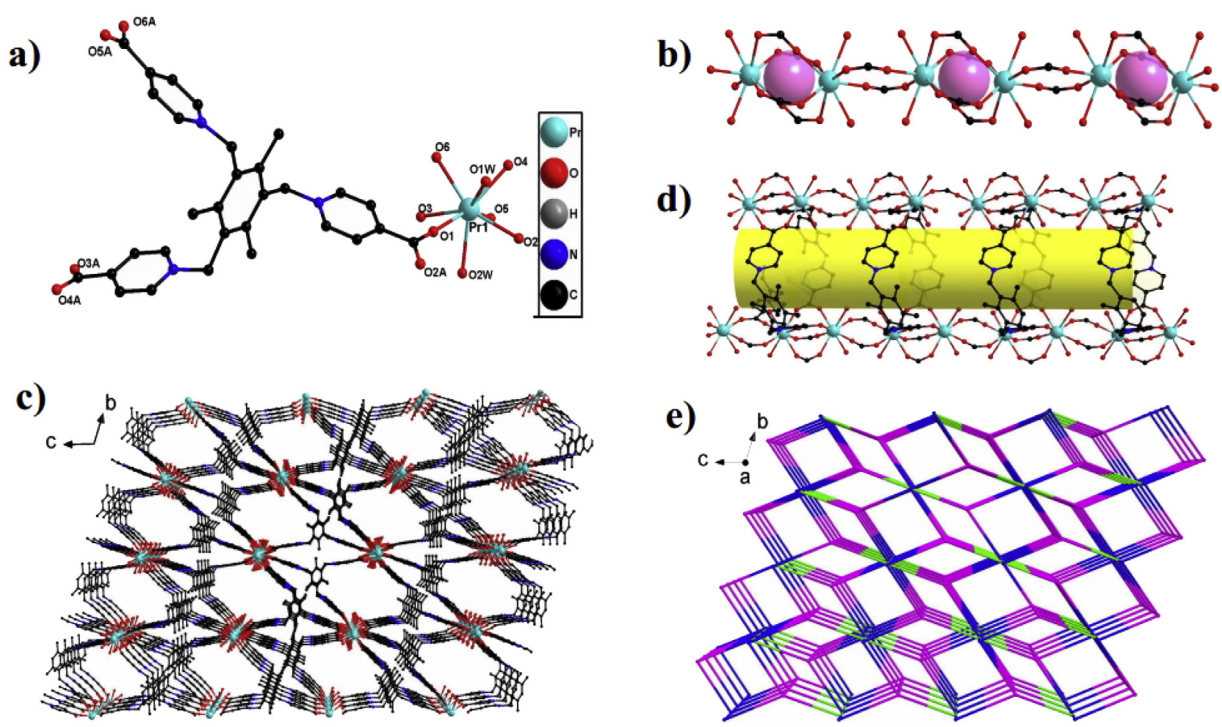

Fig. 1. (a) Diagram showing the coordination environment of Pr (III) center in **I**. (b) 1D linear metallic chain containing cavate nano-sized cages. (c) Perspective view of the 3D porous framework of **I**. (d) 1D channel in the 3D framework. (e) The 3D topological structure of **I**. (All hydrogen atoms and lattice-water molecules are omitted for clarity).

the coordination mode of μ_6-η^1:η^1:η^1:η^1:η^1:η^1:η^1 (μ_6-TTTPC^{3-}), as shown in Scheme 1. Around Pr1, the Pr–O$_{carboxy}$ bond distances for O1, O2, O3, O4, O5, and O6 atoms of TTTPC^{3-} ligands are in the range of 2.378(3) to 2.473(4) Å, which are significantly shorter than those for Pr–Ow (2.527(5) and 2.553(4) Å), indicating stronger interactions between Pr (III) center and O$_{carboxy}$ atoms. The angles of ∠O–Pr–O are within the scopes of 69.48(14)–145.50(15)°. The bond length data and angles in the present work are consistent with those in previous work covering the corresponding coordination polymers [46–50].

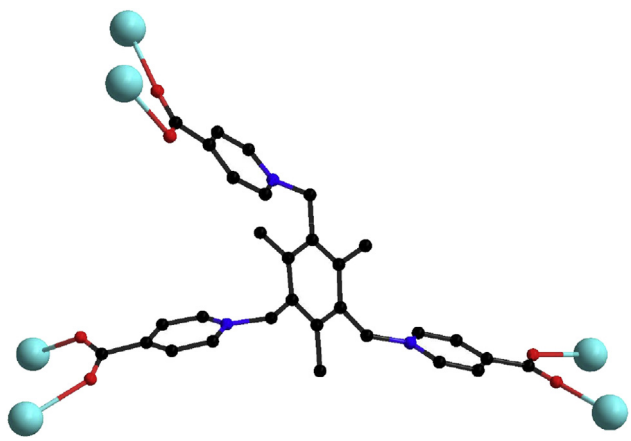

Scheme 1. The coordination mode of H_3TTTPC ligand in coordination polymers **I**, **II** and **III**.

In the framework of **I**, the closest two crystallographically equivalent Pr(III) ions are bridged by four carboxy groups (O5–C13–O6, etc.) in μ^2-η^1:η^1 fashion with the nonbonding distance of 4.369 Å (Pr…Pr) to form a cavate cage ($Pr_2(OCO)_4$), allowing to accommodate a suppositional ball with a diameter of ca. 2.930 Å, as depicted in Fig. 1b. Afterwards, based on these cage-shaped binuclear units, **I** is generated into a one-dimensional (1D) infinite linear metallic chain through the linkage of two COO^- groups end to end (see Fig. 1b). The 1D metallic chains are connected into two-dimensional (2D) layers through $TTTPC^{3-}$ ligands (see Fig. S2), which are further interlinked reciprocally along *a*-axis to give rise to a three-dimensional (3D) porous framework *via* the covalent bonding (see Fig. 1c). In the 3D architecture, 1D parallel channels with compressed hexagonal-shaped are observed along *a*-axis direction, as illustrated in Fig. 1d. The dimension of hexagonal-shaped channel is about 12.760 × 15.821 $Å^2$. The entire 3D topological structure can be simplified as shown in Fig. 1e.

As evidenced by crystallographic parameters, coordination polymers **I**, **II** and **III** are isomorphous and isostructural, and furthermore, they present regular lanthanide contraction effect. As listed in Table 2, the average distances of Ln–$O_{carboxyl}$ and Ln–Ow, cage diameters, as well as distances between cages in **I**, **II** and **III** decrease following the order of Pr, Gd and Yb, which may be attributed to the crystal field contractions of the rare earth cations lack of spherical symmetry [51,52]. Simultaneously, 4f electrons of the rare earth cations in their compounds are shielded by the $5s^2$ and $5p^6$ orbitals and therefore are scarcely available for covalent interaction with the ligands. As a result, electrostatic interactions are dominant in the rare earth elements compounds, and their geometries are determined by steric factors rather than electronic ones [53].

3.3. Luminescent properties and selective sensing of Pb^{2+} ion

Luminescent properties of lanthanide metal ions have aroused great attention because of their wide potential applications in photochemistry and sensors etc. [54–56]. Metal ion sensing and detection are significant owing to the relationship to the environment and human health of some metal ions [57–59]. Hence, much effort has been devoted to the sensing and detection of metal ions based on porosity-containing coordination polymers [60,61]. In this study, coordination polymers **II** and **III** were used to sense metal ions. In order to investigate the potential of **II** and **III** toward selectively sensing metal ions, their crystalline samples were immersed in aqueous solutions (10^{-4} M) containing various metal cations to give the metal ion incorporated suspensions of **II** and **III** for luminescence measurements. The spectra of coordination polymers **II** and **III** are similar to each other, which possess intense broad emission bands with the maximum at 392 and 391 nm upon the excitation at 243 and 244 nm and may be ascribed to intra-ligand transitions and charge transfer between the metal centers and linkers [62–65]. Emission spectra of **II** and **III** in water containing Zn^{2+}, Ag^+, Mn^{2+}, Ni^{2+}, Ca^{2+}, Cu^{2+}, Fe^{2+}, Ba^{2+}, Cd^{2+}, Co^{2+}, Pb^{2+} ions (10^{-4} M) were shown in Fig. S3 and Fig. 2, respectively. The results indicate that the tested metal ions just gave slight effect on the fluorescence intensity of the initial coordination polymer **II** (see Fig. S3). In the case of coordination polymer **III**, emission intensities of the different suspensions distinctively relate to the incorporated metal ions. The emission intensity at 391 nm decreased significantly at the presence of Pb^{2+} (10^{-4} M, $Pb(CH_3COO)_2$) ion for nearly ten times as strong as that without Pb^{2+} ion, whereas the emission intensities at 391 nm ($\lambda_{ex} = 244$ nm) only had minute degrees of quenching effects at the introductions of Zn^{2+}, Ag^+, Mn^{2+}, Ni^{2+}, Ca^{2+}, Cu^{2+}, Fe^{2+}, Ba^{2+}, Cd^{2+}, and Co^{2+} ions with respect to the original coordination polymer **III**, as illustrated in Fig. 2a.

To further identify whether coordination polymer **III** acting as a highly selective recognition sensor for Pb^{2+} ion, its anti-interference sensing ability and selectivity detection were investigated *via* the competing experiments. Some other metal ions (each 10^{-4} M) were added consecutively into a suspension of coordination polymer **III** under the same conditions. Consequently, no obvious emission intensity changes for **III** was observed at the presence of coexisting metal ions, suggesting that the quenching selectivity of **III** toward Pb^{2+} ion does not present significant interference by the introduction of the tested metal ions, which further confirms that coordination polymer **III** showing remarkable selectivity toward Pb^{2+} ion and may be considered as potential selective luminescent probes for this metal, as shown in Fig. 2b. The high selectivity for Pb^{2+} ion is probably due to several integrated factors as follows, the suitable cavity size in the frameworks of **III** and the suitable radius of the metal ions [66,67].

3.4. Magnetic analysis

Variable-temperature magnetic susceptibility of **I** was investigated in the temperature range of 2.0–300.0 K. The variation of the inverse of the magnetic susceptibility, χ_m^{-1} and $\chi_m T$ of **I** is shown in Fig. 3. The $1/\chi_m$ versus T plot of **I** is in correspondence with the Curie-Weiss law in the range of 2.0–300.0 K with $C = 0.2889$ $cm^3mol^{-1}K$ and $\theta = -407.1650$ K. At 300.0 K, the $\chi_m T$ value is 0.2572 $cm^3mol^{-1}K$ (1.434 μ_B), which is higher than the

Table 2
Comparison of the corresponding distances (Å, average) for **I**, **II** and **III**.

	I		II		III	
Bond lengths	Pr1–O	2.441	Gd1–O1	2.372	Yb1–O	2.293
	Pr1–Ow	2.546	Gd1–Ow	2.456	Yb1–Ow	2.398
Cage diameterss	2.930		3.098		3.234	
Distances between cagess	5.182		5.136		5.071	

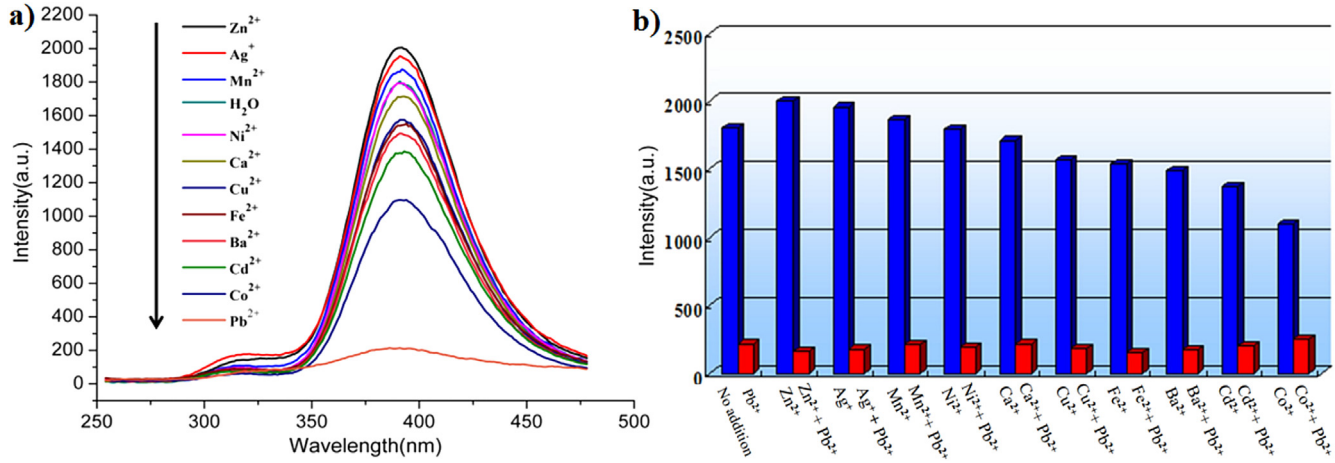

Fig. 2. (a) Emission spectra and intensities for **III** in aqueous solutions of different metal ions. (b) Luminescent intensities of **III** at 391 nm in aqueous solutions of mixed metal ions (excited at 244 nm).

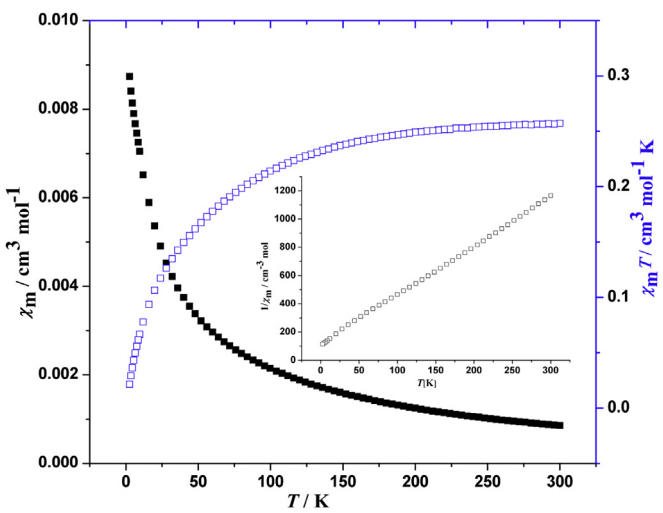

Fig. 3. Thermal variation of χ_m and $\chi_m T$ for **I**. Insert: plot of thermal variation of χ_m^{-1} for **I**.

expected value (0.1600 cm^3Kmol^{-1}, 1.131 μ_B) of isolated spin-only Pr(III) ion ($s = 1$, $g = 4/5$). As T is lowered, $\chi_m T$ decreases continuously to a value of 0.01777 $cm^3mol^{-1}K$ at 2.0 K. The negative θ value and the $\chi_m T$ vs T curve indicates a dominant antiferromagnetic interaction between the Pr(III) ions in the structures [68,69].

4. Conclusion

In summary, we report here three coordination polymers including $\{[Pr(TTTPC)\cdot(H_2O)_2]\cdot 2Cl\cdot NO_3\cdot 4H_2O\}_n$ (**I**), $\{[Gd(TTTPC)\cdot(H_2O)_2]\cdot 2Cl\cdot NO_3\cdot 4H_2O\}_n$ (**II**) and $\{[Yb(TTTPC)\cdot(H_2O)_2]\cdot 3Cl\cdot NO_3\cdot 0.5DMA\cdot 6H_2O\}_n$ (**III**) assembled by flexible ligand H_3TTTPC [1,1′,1″-(2,4,6-trimethylbenzene-1,3,5-triyl(methylene))-tris(pyridine-4-carboxylic acid)] in conventional aqueous solutions. Structural analysis indicates that they are isomorphous and isostructural, containing the unit of cavate 14-membered cages ($Ln_2(OCO)_4$) (Ln = Pr, Gd and Yb), based on which to generate a 1D infinite linear metallic chain through the linkage of two COO^- groups that are further interlinked reciprocally to polymerize into 3D porous frameworks. Magnetic analysis indicates coordination polymer **I** presents antiferromagnetism. Remarkably, the luminescent property studies demonstrate that **III** is capable of high selectivity and sensing for Pb^{2+} ion, suggesting that it may be considered as a potential selective luminescent probe towards Pb^{2+} ion.

Acknowledgments

This research is financially supported by the Natural Science Foundation of Henan Province of China (No. 162300410010 and 13A150056).

Appendix A. Supplementary data

Supplementary data related to this article can be found at http://dx.doi.org/10.1016/j.jallcom.2017.01.260.

References

[1] S. Kitagawa, Metal–organic frameworks (MOFs), Chem. Soc. Rev. 43 (2014) 5415–5418.
[2] G. Férey, Hybrid porous solids: past, present, future, Chem. Soc. Rev. 37 (2008) 191–214.
[3] N.W. Ockwig, O. Delgado-Friedrichs, M. O'Keeffe, Reticular chemistry: occurrence and taxonomy of nets and grammar for the design of frameworks, Acc. Chem. Res. 38 (2005) 176–182.
[4] W. Lu, Z. Wei, Z.Y. Gu, Tuning the structure and function of metal–organic frameworks via linker design, Chem. Soc. Rev. 43 (2014) 5561–5593.
[5] E. Iriowen, S. Orefuwa, A. Goudy, The role of sticking efficiencies in hydrogen gas adsorption on metal organic frameworks, J. Alloys Compd. 645 (2015) 242–246.
[6] H. Jasuja, G.W. Peterson, J.B. Decoste, Evaluation of MOFs for air purification and air quality control applications: ammonia removal from air, Chem. Eng. Sci. 124 (2015) 118–124.
[7] Y. He, W. Zhou, G. Qian, Methane storage in metal–organic frameworks, Chem. Soc. Rev. 43 (2014) 5657–5678.
[8] S. Hasegawa, S. Horike, R. Matsuda, Three-dimensional porous coordination polymer functionalized with amide groups based on tridentate ligand: selective sorption and catalysis, J. Am. Chem. Soc. 129 (2007) 2607–2614.
[9] J.Y. Lee, O.K. Farha, J. Roberts, Metal–organic framework materials as catalysts, Chem. Soc. Rev. 38 (2009) 1450–1459.
[10] V. Chandrasekhar, S. Hossain, S. Das, Rhombus-shaped tetranuclear [Ln_4] complexes [Ln = Dy (III) and Ho (III)]: synthesis, structure, and SMM behavior, Inorg. Chem. 52 (2013) 6346–6353.
[11] V. Stavila, A.A. Talin, M.D. Allendorf, MOF–based electronic and optoelectronic devices, Chem. Soc. Rev. 43 (2014) 5994–6010.
[12] R. Perumal, S.M. Babu, Synthesis, crystalline perfection, optical and dielectric studies on metal–organic tri-allylthiourea cadmium chloride (ATCC) nonlinear optical single crystal by solution growth technique, J. Alloys Compd. 538 (2012) 131–135.
[13] S. Loera-Serna, M.A. Oliver-Tolentino, M. de Lourdes López-Núñez, Electrochemical behavior of [$Cu_3(BTC)_2$] metal–organic framework: the effect of the method of synthesis, J. Alloys Compd. 540 (2012) 113–120.

[14] Z. Hu, B.J. Deibert, J. Li, Luminescent metal–organic frameworks for chemical sensing and explosive detection, Chem. Soc. Rev. 43 (2014) 5815–5840.
[15] Z.J. Lin, B. Xu, T.F. Liu, A series of lanthanide metal–organic frameworks based on biphenyl-3,4′,5-tricarboxylate: syntheses, structures, luminescence and magnetic properties, Eur. J. Inorg. Chem. 24 (2010) 3842–3849.
[16] B.D. Chandler, J.O. Yu, D.T. Cramb, Series of lanthanide-alkali metal–organic frameworks exhibiting luminescence and permanent microporosity, Chem. Mater. 19 (2007) 4467–4473.
[17] H. Guo, Y. Zhu, S. Qiu, Coordination modulation induced synthesis of nanoscale Eu1–xTbx–Metal–Organic frameworks for luminescent thin films, Adv. Mater. 22 (2010) 4190–4192.
[18] J.Y. Wu, T.T. Yeh, Y.S. Wen, Unusual robust luminescent porous frameworks self–assembled from lanthanide ions and 2,2′-bipyridine-4,4′-dicarboxylate, Cryst. Growth Des. 6 (2006) 467–473.
[19] L. Yang, L. Liu, L. Wu, A series of 3D isomorphous lanthanide coordination polymers based on flexible dicarboxylate ligand: synthesis, structure, characterization, and properties, Dyes Pigments 105 (2014) 180–191.
[20] J. Xu, J. Cheng, W. Su, Effect of lanthanide contraction on crystal structures of three-dimensional lanthanide based metal–organic frameworks with thiophene-2,5-dicarboxylate and oxalate, Cryst. Growth Des. 11 (2011) 2294–2301.
[21] Y.Q. Sun, J. Zhang, Y.M. Chen, Porous lanthanide–organic open frameworks with helical tubes constructed from interweaving triple-helical and double-helical chains, Angew. Chem. 117 (2005) 5964–5967.
[22] V. Guillerm, D. Kim, J.F. Eubank, A supermolecular building approach for the design and construction of metal–organic frameworks, Chem. Soc. Rev. 43 (2014) 6141–6172.
[23] M. O'Keeffe, Design of MOFs and intellectual content in reticular chemistry: a personal view, Chem. Soc. Rev. 38 (2009) 1215–1217.
[24] J.J. Perry Iv, J.A. Perman, M.J. Zaworotko, Design and synthesis of metal–organic frameworks using metal–organic polyhedra as supermolecular building blocks, Chem. Soc. Rev. 38 (2009) 1400–1417.
[25] D.J. Tranchemontagne, J.L. Mendoza-Cortés, M. O'Keeffe, Secondary building units, nets and bonding in the chemistry of metal–organic frameworks, Chem. Soc. Rev. 38 (2009) 1257–1283.
[26] Z. Lu, H. Xing, R. Sun, Water stable metal–organic framework evolutionally formed from a flexible multidentate ligand with acylamide groups for selective CO_2 adsorption, Cryst. Growth Des. 12 (2012) 1081–1084.
[27] X.H. Wei, L.Y. Yang, S.Y. Liao, A series of rare earth complexes with novel non-interpenetrating 3D networks: synthesis, structures, magnetic and optical properties, Dalton Trans. 43 (2014) 5793–5800.
[28] X. Rui, Q.Z. Zha, T.T. Wei, Syntheses and crystal structures of coordination polymers of a porphyrin ligand bearing two pyridyl and two carboxyl moieties, Inorg. Chem. Commun. 48 (2014) 111–113.
[29] X.H. Zhang, Z.J. Zhang, D.H. Xie, Synthesis and supercapacitor application of nanoporous carbon by the direct carbonization of aluminium salicylate coordination polymer, J. Alloys Compd. 607 (2014) 23–31.
[30] T.T. Li, S.L. Cai, R.H. Zeng, Structures and luminescent properties of two new main group coordination polymers based on 2-(hydroxymethyl)-1H-imidazole-4,5-dicarboxylic acid, Inorg. Chem. Commun. 48 (2014) 40–43.
[31] W. Zhang, J. Yu, Y. Cui, Assembly and tunable luminescence of lanthanide-organic frameworks constructed from 4-(3,5-dicarboxyphenyl) pyridine-2,6-dicarboxylate ligand, J. Alloys Compd. 551 (2013) 616–620.
[32] L. Yang, L. Wu, H. Zhang, Synthesis, structure and luminescent recognition properties of cerium (IV) coordination polymers based on pyridine-2,6-dicarboxylic acid, Dyes Pigments 99 (2013) 257–267.
[33] L. Yang, L. Wu, L. Liu, Three novel transition metal coordination polymers based on (2,3-f)-pyrazino (1,10) phenanthroline-2,3-dicarboxylic acid sodium salt: hydrothermal syntheses, structures, and properties, Dyes Pigments 101 (2014) 196–202.
[34] Y. He, B. Li, M. O'Keeffe, Multifunctional metal–organic frameworks constructed from meta-benzenedicarboxylate units, Chem. Soc. Rev. 43 (2014) 5618–5656.
[35] J.Z. Gu, A.M. Kirillov, J. Wu, Synthesis, structural versatility, luminescent and magnetic properties of a series of coordination polymers constructed from biphenyl-2,4,4′-tricarboxylate and different N-donor ligands, CrystEngComm 15 (2013) 10287–10303.
[36] B. Zhao, X.Y. Chen, P. Cheng, Coordination polymers containing 1D channels as selective luminescent probes, J. Am. Chem. Soc. 126 (2004) 15394–15395.
[37] T. Ma, M.X. Li, Z.X. Wang, Structural diversity, luminescence, and magnetic properties of eight Co(II)/Zn(II) coordination polymers constructed from semirigid ether–linked tetracarboxylates and bend dipyridyl-triazole ligands, Cryst. Growth Des. 14 (2014) 4155–4165.
[38] D.X. Hu, F. Luo, Y.X. Che, Construction of lanthanide metal-organic frameworks by flexible aliphatic dicarboxylate ligands plus a rigid m-phthalic acid ligand, Cryst. Growth Des. 7 (2007) 1733–1737.
[39] R. Ding, P. Yan, G. Hou, A novel 3D 4-(1H-1,2,4-triazol-1-ylmethyl) benzoate cadmium coordination polymer, Synth. Met. 162 (2012) 1894–1897.
[40] A. Schneemann, V. Bon, I. Schwedler, Flexible metal–organic frameworks, Chem. Soc. Rev. 43 (2014) 6062–6096.
[41] J.K. Gregory, D.C. Clary, K. Liu, The water dipole moment in water clusters, Science 275 (1997) 814–817.
[42] X. Zou, M. Li, P. Yan, Systematic study on the structures of salen type lanthanide complexes tuned by lanthanide contraction and corresponding luminescence, Dalton Trans. 42 (2013) 9482–9489.
[43] X.F. Li, Z.B. Han, X.N. Cheng, Studies on the radii dependent lanthanide self–assembly coordination behaviors of a flexible dicarboxylate ligand, Inorg. Chem. Commun. 9 (2006) 1091–1095.
[44] H. Bai, Z. Wu, M. Hu, Lanthanide metal–organic frameworks with 2, 2′-bipyridine-polycarboxylic acid: synthesis, crystal structures and fluorescent properties, Inorg. Chim. Acta 427 (2015) 112–117.
[45] L.R. Yang, S. Song, H.M. Zhang, Synthesis, characterization and thermal decomposition kinetics as well as evaluation of luminescent properties of several 3D lanthanide coordination polymers as selective luminescent probes of metal ions, Synth. Met. 162 (2012) 1775–1788.
[46] J. Zhu, H.F. Song, P.F. Yan, Slow relaxation processes of salen type Dy_2 complex and 1D ionic spiral Dy_n coordination polymer, CrystEngComm 15 (2013) 1747–1752.
[47] A. Abbasi, F. Mohammadnezhad, S.A. Geranmayeh, Novel 3–d nanoporous Ce (III) metal–organic framework with terephthalic acid; thermal, topology, porosity and structural studies, J. Inorg. Organomet. Polym. 24 (2014) 1021–1026.
[48] B. Zhao, P. Cheng, Y. Dai, A nanotubular 3D coordination polymer based on a 3d–4f heterometallic assembly, Angew. Chem. Int. Ed. 42 (2003) 934–936.
[49] P. Silva, L. Cunha-Silva, N.J.O. Silva, Metal–organic frameworks assembled from erbium tetramers and 2,5-pyridinedicarboxylic acid, Cryst. Growth Des. 13 (2013) 2607–2617.
[50] S.L. Li, Y.Q. Lan, J.C. Ma, Metal–Organic frameworks based on different benzimidazole derivatives: effect of length and substituent groups of the ligands on the structures, Cryst. Growth Des. 10 (2010) 1161–1170.
[51] J. Yao, B. Deng, L.J. Sherry, Syntheses, structure, some band gaps, and electronic structures of CsLnZnTe3 (Ln = La, Pr, Nd, Sm, Gd, Tb, Dy, Ho, Er, Tm, Y), Inorg. Chem. 43 (2004) 7735–7740.
[52] Y.Q. Sun, G.Y. Yang, Organic–inorganic hybrid materials constructed from inorganic lanthanide sulfate skeletons and organic 4, 5-imidazoledicarboxylic acid, Dalton Trans. 34 (2007) 3771–3781.
[53] L. Armelao, S. Quici, F. Barigelletti, Design of luminescent lanthanide complexes: from molecules to highly efficient photo–emitting materials, Coord. Chem. Rev. 254 (2010) 487–505.
[54] Qin, B. Ma, X.F. Liu, Aqueous-and vapor-phase detection of nitroaromatic explosives by a water-stable fluorescent microporous MOF directed by an ionic liquid, J. Mater. Chem. A 3 (2015) 12690–12697.
[55] Z. Hao, X. Song, M. Zhu, One-dimensional channel-structured Eu-MOF for sensing small organic molecules and Cu^{2+} ion, J. Mater. Chem. A 1 (2013) 11043–11050.
[56] X.Y. Dong, M. Zhang, R.B. Pei, A crystalline copper (II) coordination polymer for the efficient visible-light-driven generation of hydrogen, Angew. Chem. Int. Ed. 55 (2016) 2073–2077.
[57] M. Formica, V. Fusi, L. Giorgi, New fluorescent chemosensors for metal ions in solution, Coord. Chem. Rev. 256 (2012) 170–192.
[58] D. Huang, C. Niu, M. Ruan, Highly sensitive strategy for Hg^{2+} detection in environmental water samples using long lifetime fluorescence quantum dots and gold nanoparticles, Environ. Sci. Technol. 47 (2013) 4392–4398.
[59] S.S. Zhao, J. Yang, Y.Y. Liu, Fluorescent aromatic tag–functionalized MOFs for highly selective sensing of metal ions and small organic molecules, Inorg. Chem. 55 (2016) 2261–2273.
[60] Y. You, S. Cho, W. Nam, Cyclometalated iridium (III) complexes for phosphorescence sensing of biological metal ions, Inorg. Chem. 53 (2013) 1804–1815.
[61] X.Y. Dong, R. Wang, J.Z. Wang, Highly selective Fe^{3+} sensing and proton conduction in a water-stable sulfonate–carboxylate Tb–organic–framework, J. Mater. Chem. A 3 (2015) 641–647.
[62] P.R. Matthes, J. Nitsch, A. Kuzmanoski, The series of rare earth complexes $[Ln_2Cl_6$ (μ-4,4′-bipy)$(py)_6]$, Ln = Y, Pr, Nd, Sm–Yb: a molecular model system for luminescence properties in MOFs based on $LnCl_3$ and 4,4′-bipyridine, Chem. Eur. J. 19 (2013) 17369–17378.
[63] Y. Cui, Y. Yue, G. Qian, Luminescent functional metal–organic frameworks, Chem. Rev. 112 (2011) 1126–1162.
[64] P. Wang, J.P. Ma, Y.B. Dong, Tunable luminescent lanthanide coordination polymers based on reversible solid-state ion-exchange monitored by ion-dependent photoinduced emission spectra, J. Am. Chem. Soc. 129 (2007) 10620–10621.
[65] M.D. Allendorf, C.A. Bauer, R.K. Bhakta, Luminescent metal–organic frameworks, Chem. Soc. Rev. 38 (2009) 1330–1352.
[66] P. Wu, Y. Liu, Y. Liu, Cadmium-based metal–organic framework as a highly selective and sensitive ratiometric luminescent sensor for mercury (II), Inorg. Chem. 54 (2015) 11046–11048.
[67] D. Wu, W. Huang, Z. Lin, Highly sensitive multiresponsive chemosensor for selective detection of Hg^{2+} in natural water and different monitoring environments, Inorg. Chem. 47 (2008) 7190–7201.
[68] X. Feng, X.L. Ling, L. Liu, A series of 3D lanthanide frameworks constructed from aromatic multi-carboxylate ligand: structural diversity, luminescence and magnetic properties, Dalton Trans. 42 (2013) 10292–10303.
[69] C. Benelli, D. Gatteschi, Magnetism of lanthanides in molecular materials with transition–metal ions and organic radicals, Chem. Rev. 102 (2002) 2369–2388.